Cooperative Decentralized Intersection Collision Avoidance Using Extended Kalman Filtering

Ashil Sayyed Farahmand and Lamine Mili, *Member, IEEE*

***Abstract*—Vehicle accidents are a major cause of death and claim more than 40,000 lives annually in the US alone. A substantial portion of these accidents occur at intersections. Stop signs and traffic signals are some of the intersection control devices used to increase safety and prevent collisions. However, these devices themselves can contribute to collisions, are costly, inefficient, and are prone to failure. This paper proposes an adaptive, decentralized, cooperative collision avoidance (CCA) system that optimizes each vehicle's controls subject to the constraint that no collisions occur. Three major contributions to the field of collision avoidance have resulted from this research. First, a nonlinear 5-state variable vehicle model is expanded from an earlier one developed in [2]. Second, a set of constrained, coupled Extended Kalman Filters (EKF) are used to predict vehicular trajectory in real-time. Third, a vehicular network based on the new WAVE standard is presented that provides cooperative capabilities by enabling intervehicle communication. The system is simulated against today's common intersection control devices and is shown to be superior in minimizing average vehicle delay.**

I. Introduction

Intersection collision avoidance is attracting more interest from the research community as technological advances make it possible to improve on the performance of stop signs and traffic signals using new intersection control devices. Currently, stop signs and traffic signals can become hazardous in a number of ways.

Stop signs and traffic signals are unsafe since they rely on physical infrastructure. Stop signs are at risk of being knocked down by inconsiderate teenagers. On one occasion, a sign was illegally dismantled six times in only 17 days resulting in a fatal, high speed accident [3]. Both devices are also susceptible to foul weather. Furthermore, a traffic signal's reliance on the electric grid makes it vulnerable to power outages.

Stop signs and traffic signals are inefficient since they are unable to appropriately adapt to changing traffic conditions. Stop signs require each vehicle to come to a complete stop even if a long line of vehicles are coming from one approach. Although the intersection is able to support a smooth flow of the same number of vehicles in far less time, the stop sign's stopping requirement introduces unnecessary delay to the drivers. Traffic signals can also introduce unnecessary delay since drivers need time to react to signal transitions.

Researchers have generally attempted to propose two types of intersection control technologies, optical and cooperative systems. Optical collision avoidance systems use image processing to identify objects on a roadway. The objects are then tracked to estimate their dynamics and warn the drivers if a collision may occur. Optical systems are generally used for lane-keeping [5], observation of pedestrians [4], [7], and navigating urban environments [6].

Cooperative systems generally rely on roadway and vehicular sensors to obtain data then use wireless communication to share that information. These systems have been applied to collision avoidance at blind crossings [8] and to transmit information about upcoming hazards to a driver approaching a curved roadway [9] in addition to other applications.

Although optical and cooperative systems are designed to improve safety, they each have their shortcomings. The reliance on line-of-sight currently limits vehicle-mounted optical cameras to little more than warning devices since the intersection cannot fully be viewed until the vehicle has entered it. The use of cooperative collision avoidance in the near future is hindered by the need for more infrastructure and other issues. This includes transceivers for every vehicle and in some cases, roadside transceivers as well. If any vehicle does not transmit information or transmits wrong information, the system as a whole can fail [10].

The research conducted in this paper seeks to improve upon the performance of current intersection control devices - specifically traffic signals and stop signs - by proposing an adaptive, decentralized, cooperative collision avoidance system that acts as a traffic signal in dense traffic and as a yield sign in sparse traffic. The system's adaptive nature allows it to operate efficiently under a range of traffic conditions while decentralization allows operation independent of any outdoor, physical infrastructure. Vehicles use low-cost wireless equipment along with the new IEEE 1609 family of standards to cooperatively negotiate safe routes as opposed to using costly traffic signals and inefficient stop signs.

The system has each vehicle measure its position using GPS and its other state information using internal sensors. The state information of all vehicles is shared on a wireless network. The observations of all vehicles are passed to a set

Manuscript received December 23, 2008.

A. S. Farahmand is with the Bradley Department of Electrical and Computer Engineering at Virginia Polytechnic Institute and State University, Blacksburg, VA 24061 USA (phone: 571-270-7079; e-mail: asfarahm@vt.edu)

L. Mili is with the Bradley Department of Electrical and Computer Engineering at Virginia Polytechnic Institute and State University, Blacksburg, VA 24061 USA (e-mail: lmili@vt.edu)

of constrained, coupled Extended Kalman Filters (EKF). The filtered state information is used to determine the optimal trajectory each vehicle should take through the intersection in order to minimize the average delay experienced by all vehicles. To ensure compliance with the optimization results, the vehicles' controls then become automated until the intersection is traversed.

Each vehicle is modelled with a nonlinear state-space model that accounts for vehicular dynamics and internal engine parameters. This model improves on idealized, linear tracker models that only account for position, velocity, and acceleration by allowing state dependent frictional forces arising from the engine and environment to be considered. In addition, the model allows the optimization to solve the fundamental problem of finding the optimal set of vehicular controls as opposed to the tracker model, which only yields a solution in terms of acceleration. The tracker model can be made comparable to the nonlinear vehicle model used here only if the acceleration is a function of the vehicle's state vector.

The proposed system is only a first step and is not ready to be implemented in its current form but makes 3 major contributions to the field of collision avoidance: a nonlinear vehicle state-space model, a constrained EKF, and a vehicular network for control at intersections. These contributions are detailed in this paper. The system is simulated against stop signs and traffic signals and the results are described.

This paper is organized as follows. In section 2, the nonlinear vehicle model is presented. In section 3, the implementation of the EKF is discussed. In section 4, the vehicular network and optimization algorithm is described. In section 5, simulation results are presented. Conclusions and future research are discussed in section 6.

II. Vehicle State-Space Model

The vehicle model is based on tabulated data for a 1990 Lincoln Town Car. It is an expanded form of one derived in [2] with portions from other sources. The vehicle modelled herein is a typical 6-cylinder, front-wheel drive car with a Ford AOD transmission and a continuous, four-stroke, naturally-aspirated, spark-ignition engine. For a detailed presentation of powertrains in general, the reader is referred to [1].

This model expands upon the original and consists of 3 control and 5 state variables. The vehicle's controls are the throttle angle α, the brake angle β, and the steering angle θ. The throttle and brake angles are defined from 0-85^{O} while the steering angle ranges from 0-360^{O}. A vehicle travelling at a steering angle of 0^{O} is defined as moving toward the positive-x_1 axis. The state variables are composed of the x_1 and x_2 position coordinates, the mass of air in the intake manifold m_a, the engine angular velocity ω_e, and the brake torque T_b. The model assumes that all movement is only in 2 dimensions.

The governing equation for the mass of air in the intake manifold is determined by balancing the mass flow rates of air entering and exiting the intake manifold and is given by

$$\dot{m}_a = c_{mfr} n_{tc} n_{pif} - c_1 \eta_{vol} m_a \omega_e , \qquad (1)$$

where c_{mfr} is defined as the maximum flow rate of air corresponding to a fully opened throttle valve, n_{tc} determines the influence of the throttle angle on the mass flow rate of air entering the intake manifold, n_{pif} represents the effect the pressure difference between intake manifold and the atmosphere has on the incoming mass flow rate of air, c_1 is a engine-dependent constant, and η_{vol} is defined as the volumetric efficiency of the engine.

The engine angular velocity is determined using Newton's Laws and is given as the solution of

$$\dot{\omega}_e = \frac{T_i - T_f - T_p - T_l}{J_e^*} , \qquad (2)$$

where the indicated engine torque T_i represents the gross power generated by combustion in the engine cylinders, T_f models internal engine and powertrain losses, T_p accounts for losses in the torque converter, the load torque T_l accounts for losses due to the brakes, the rolling resistance of the vehicle, and aerodynamic drag, while J_e^* is vehicle and gear-dependent constant.

The brake torque is described by the linear differential equation

$$\dot{T}_b = \frac{K_b \beta - T_b}{\tau_{b,v}} , \qquad (3)$$

where K_b is the brake torque constant of proportionality and $\tau_{b,v}$ is the brake time constant.

These equations will now be put into vector-matrix form and an EKF will be used to estimate the states from noisy measurements.

III. Extended Kalman Filter Implementation

A set of constrained, coupled, recursive EKFs are used to estimate vehicle trajectories to provide accurate estimates for use in the optimization. In this section, the theoretical foundations and implementation details for each vehicle's filter are discussed.

The EKF estimates the state information of nonlinear, dynamic systems. At each time step, it predicts the next state of the system using all past observations, receives a new noisy observation, then makes a filtered estimate of the system's state by processing both the new observation and

the prediction. The filter's state and observation equations are given by

$$\dot{\underline{x}}(t) = \underline{f}\left(\underline{x}(t), \underline{u}(t), t\right) + \underline{w}(t), \quad (4)$$

$$\underline{z}(t) = \underline{h}\left(\underline{x}(t), \underline{u}(t), t\right) + \underline{e}(t) \quad t = t_i \quad i = 1,2..., \quad (5)$$

respectively, where $\underline{x}(t)$ is the state vector, $\underline{u}(t)$ is the control vector, $\underline{f}$ is the vehicle state equations, $\underline{w}(t)$ is the process noise, $\underline{z}(t)$ is the observation vector, and $\underline{e}(t)$ is the observation noise with covariance $\underline{R}(t)$. Both $\underline{f}$ and $\underline{h}$ are functions that are continuous and continuously differentiable with respect to all elements of $\underline{x}(t)$ and $\underline{u}(t)$. It is assumed that the state equation is continuous and that the observations are made at discrete intervals. It is also assumed that $\underline{u}(t)$ is known and does not change during one time interval.

The filter predicts the next state of the system by integrating $\underline{f}$ from the time of the last filtered estimate to the time of prediction and is expressed as

$$\hat{\underline{x}}_{k|k-1} = \hat{\underline{x}}_{k-1|k-1} + \int_{t_{k-1}}^{t_k} \underline{f}\left(\hat{\underline{x}}(t \mid t_{k-1}), \underline{u}^*(t), t\right) dt, \quad (6)$$

where $\underline{u}^*(t)$ is the nominal control vector. It is assumed that the following nominal trajectories are known:

$$\dot{\underline{x}}^*(t) = \underline{f}\left(\underline{x}^*(t), \underline{u}^*(t), t\right), \quad (7)$$

$$\underline{z}^*(t) = \underline{h}\left(\underline{x}^*(t), \underline{u}^*(t), t\right). \quad (8)$$

At the first time step, the initial conditions serve as $\underline{x}^*(t)$, our nominal states; for subsequent steps, the previous step's filtered estimate is used. The nominal controls are equivalent to $\underline{u}(t)$. Since $\underline{f}$ does not have an analytical solution in our case, the 4th order Runge-Kutta method is used to approximate the solution. In order to maintain physically realizable solutions, the following constraints are imposed on the predictions: $m_a \geq 10^{-10}$ kg, $T_b \geq 0\ N \cdot m$, $\omega_e \geq$ 6.5 rad/s when $\beta = 0^0$, and $\omega_e \geq 10^{-5}$ rad/s when $\beta > 0^0$.

After the prediction stage, the filter receives a new observation. Since the vehicle velocity is dependent on ω_e, which is a function of m_a and T_b, all states need to be directly observed.

The EKF linearizes the system around the last filtered estimate, discretizes the result, then uses the new discretized, linear perturbation equations in conjunction with the prediction and observations to compute a new filtered estimate of the system state at the next time step. The discretized, linear perturbation state and observation equations are expressed as

$$\delta \underline{x}_k = \underline{\phi}_{k,k-1} \delta \underline{x}_{k-1} + \underline{w}_{d;k-1}, \quad (9)$$

$$\delta \underline{z}_k = \underline{H}_{x;k} \delta \underline{x}_k + \underline{e}_k, \quad (10)$$

respectively, where

$$\delta \underline{x}_k = \underline{x}_k - \underline{x}_k^*, \quad (11)$$

$$\underline{\phi}_{k,k-1} = e^{\underline{F}_x T}, \quad (12)$$

$$\underline{F}_x = \left. \frac{\partial \underline{f}\left(\underline{x}(t), \underline{u}(t), t\right)}{\partial \underline{x}} \right|_{\underline{x}(t)=\underline{x}^*(t), \underline{u}(t)=\underline{u}^*(t)}, \quad (13)$$

$$\underline{H}_x = \left. \frac{\partial \underline{h}\left(\underline{x}(t), \underline{u}(t), t\right)}{\partial \underline{x}} \right|_{\underline{x}(t)=\underline{x}^*(t), \underline{u}(t)=\underline{u}^*(t)} = \underline{I}, \quad (14)$$

and

$$E[\underline{w}_{d;k-1} \underline{w}_{d;k-1}^T] = \underline{Q}_{d;k-1}. \quad (15)$$

Assuming $\underline{F}_X$ and $\underline{Q}(t)$ are approximately constant over one interval, $\underline{Q}_{d;k} = \underline{Q}_{d;k-1} T$. The filtered estimate is given by

$$\hat{\underline{x}}_{k|k} = \hat{\underline{x}}_{k|k-1} + \underline{K}_k \left\{ \underline{z}_k - \hat{\underline{x}}_{k|k-1} \right\}, \quad (16)$$

where the gain is expressed as

$$\underline{K}_k = \underline{\sum}_{k|k-1} \left(\underline{\sum}_{k|k-1} + \underline{R}_k \right)^{-1}. \quad (17)$$

The predicted state error is given by

$$\underline{\sum}_{k|k-1} = \underline{\phi}_{k|k-1} \underline{\sum}_{k-1|k-1} \underline{\phi}_{k|k-1}^T + \underline{Q}_{d;k}. \quad (18)$$

After filtering, the covariance of the updated state error is given by

$$\underline{\sum}_{k|k} = \left[\underline{I} - \underline{K}_k \right] \cdot \underline{\sum}_{k|k-1}. \quad (19)$$

The same constraints placed on the state predictions are applied to the filtered estimates as well.

The estimated errors are further minimized by iterating the filtering stage. After computing $\underline{Q}_{d;k}$, the filter iterates by linearizing and discretizing (4) around the filtered estimate of the last iteration, then by recalculating $\underline{F}_x\left(\underline{x}^*(t), \underline{u}^*(t), t\right)$, $\underline{\phi}_{k,k-1}$, $\underline{\sum}_{k|k-1}$, $\underline{K}_k$, and $\hat{\underline{x}}_{k|k}$. The iterative form of the EKF filtering equation is expressed as

$$\underline{x}_{k|k}^{(i+1)} = \hat{\underline{x}}_{k|k-1} + \underline{K}_k^{(i)} \left\{ \underline{z}_k - \hat{\underline{x}}_{k|k-1} \right\}, \quad (20)$$

where the gain is a function of the filtered estimate from the previous iteration. Once the highest valued element of the absolute difference between two consecutive filtered state vector estimates is within an error of 10^{-6}, the iterations cease. Afterwards, $\underline{\sum}_{k|k}$ is calculated.

Each vehicle constructs a coupled EKF by lumping

together information from different vehicles. In a two vehicle system, the coupled state vector is defined by having the state variables for vehicle 2 follow those of vehicle 1 such that the sixth element of $\underline{x}$ is the x_1 coordinate of second vehicle. Other coupled vectors and matrices are similarly defined. An EKF update frequency of 1 kHz is chosen to ensure good estimates until vehicles clear the intersection.

IV. Sparse Traffic Optimization Algorithm

The sparse traffic optimization algorithm uses the coupled EKF's estimates to determine the optimal set of controls for each vehicle by minimizing the average delay of the vehicles approaching the intersection. The delay is defined as the amount of additional time required for a vehicle to traverse the intersection due to the priority of other vehicles being yielded the right-of-way and is given by the objective function

$$\arg\min \tau = \frac{1}{n}\sum_{k=1}^{n}\left(t_{o,k} - t_{a,k}\right), \qquad (21)$$

where τ is defined as the average delay, n is the number of vehicles, $t_{o,k}$ is the amount of time taken for the k-th vehicle to cross the intersection according to the result of the optimization algorithm, and $t_{a,k}$ is the amount of time taken for the k-th vehicle to cross the intersection if no other vehicles are present. The process used by the algorithm to calculate these times is discussed in the remainder of this section. The optimization represents each vehicle as a circle with a known, fixed radius that is dependent on the vehicle size. The minimization is subject to the constraint

$$(x_{1,j} - x_{1,i})^2 + (x_{2,j} - x_{2,i})^2 > (R_i + R_j + m_s)^2, \qquad (22)$$

where $x_{1,j}$ is defined as the x_1 position of the center of the j-th vehicle, R_i is the radius of the i-th vehicle, and m_s is the system safety margin. This constraint forces the optimization algorithm to maintain a safe distance between each pair of vehicles. The intersection is assumed to be square with four single lane approaches. The optimization algorithm's view of a two vehicle scenario is illustrated in Figure 1.

The operation of the algorithm generally emulates that of a yield sign. Whenever two vehicles approach an intersection, the vehicle that is able to traverse the intersection first if the other vehicle is not present is given the right-of-way. The other vehicle must cross the intersection after the first. The algorithm works similarly for multiple vehicles by forcing lower priority vehicles to delay in order to allow preceding vehicles to cross.

The algorithm begins by choosing a particular order for the vehicles to cross the intersection. A procedure for determining all possible combinations is presented by Li and Wang [8]. Next, $t_{a,k}$ and $t_{o,k}$ are calculated by predicting a vehicle's future trajectory based on its current states and intended direction. Prediction involves integrating the vehicle's state equations. A piecewise constant approximation for the vehicle acceleration is derived through simulations. To account for discrepancies between the approximated and real accelerations, the system safety margin has been included in (22). The approximation is discussed in [1].

$t_{a,k}$ and $t_{o,k}$ are determined by recognizing that all vehicles perform certain common actions. If a vehicle is going straight, it will accelerate to the maximum allowed speed, and then keep that speed. If turning, it will first accelerate, then slow down at a brake angle of 37.6696^0, then change its steering angle at a constant, uniform rate as it enters the intersection, then accelerate once again when exiting. All accelerations occur with a throttle angle of 85^0 and vehicles keep a constant speed on turns. The algorithm computes $t_{a,k}$ by simulating the time it takes for each vehicle to cross the intersection.

Whenever a vehicle has begun braking in preparation for a turn, the vehicle's controls will no longer be changed if the optimization algorithm is run again. Since the range of WAVE is sufficient to find vehicles 1 km away, it is assumed that any vehicles that could possibly collide with a vehicle this near have already been accounted for.

Lower priority vehicles repeat the above procedure but perform a safety check at the end. The vehicle checks to see if its optimal path violates the minimum distance constraint between itself and all higher priority vehicles. If the optimization is within the constraints and a collision does

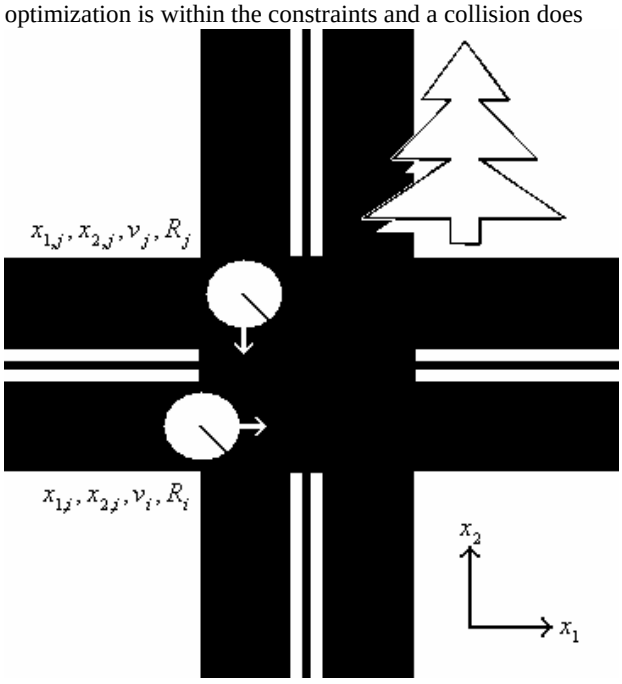

Fig. 1 Illustration of Optimization Variables

not occur, the set of controls are kept and the next vehicle is optimized. Otherwise, the optimization is run again but is preceded by a delay phase. The vehicle's maximum allowed initial velocity is reduced by 0.5 MPH from the speed limit in this phase. If the vehicle's initial velocity is above this new limit, it will be forced to depress the brake at an angle of 19^0 until reaching this speed before optimizing again. If this optimization still results in a collision, then the maximum allowed initial velocity is reduced by another 0.5 MPH. Adjusting this value of 0.5 MPH upwards results in a faster algorithm. However, it also means that the vehicles may be slowing down more than needed and therefore, introducing more delay. The value chosen here strikes a balance between these design considerations. The process of optimizing and reducing speed is repeated until a collision free trajectory is produced. The time required to complete the collision free path is recorded. Note that $t_{a,k}$ and $t_{o,k}$ will be the same for each vehicle unless this delay phase is required.

The difference between the collision free time and the optimal time determines a vehicle's delay. The average delay of all vehicles determines the cost of the particular vehicle ordering used. All possible vehicle order combinations are applied to the optimization algorithm and the one yielding the minimum cost is chosen. If two combinations have identical costs, the one that prioritizes the vehicles with lower valued globally unique MAC addresses will be chosen. Notice, however, that the number of combinations increases rapidly as more vehicles are included. Since the maximum range of WAVE is 1 km and the speeds of the vehicles being optimized are near 50 MPH, the optimization algorithm only has approximately 22 seconds to make a decision in the worst case scenario. In the implementation of a traffic optimization algorithm, the performance of the optimization must be balanced with the required processing time. The number of combinations that must be considered along with the time intensive nature of the optimization make this algorithm unsuitable for dense traffic. Therefore, a limit of 5 vehicles has been allowed for the sparse traffic optimization algorithm.

The dense traffic optimization algorithm is designed to make decisions with less information and less time than its sparse counterpart. The sparse algorithm assumes the vehicle network is fully meshed so each vehicle is able to communicate and receive information from every other vehicle. However, the network congestion created by many communicating vehicles means this configuration is difficult to achieve in dense traffic. The sparse algorithm converts to the dense algorithm when the number of vehicles exceeds 5. The dense algorithm is used when the sparse algorithm is unlikely to be executed quickly enough or is unlikely to be supported by the network. Currently, the dense traffic optimization algorithm is underdeveloped and is in need of further research. Readers are referred to [1] for a description of this algorithm in its present form.

V. Simulation Results

The performance of the sparse traffic optimization algorithm is evaluated by comparing it against conventional intersection control devices. The delay of this algorithm is compared to the delay introduced by a stop sign and a typical traffic signal. The simulations occur at a four approach, single lane intersection with 3.6 m wide lanes.

The stop sign is compared to the optimization algorithm in five simulations. The purpose of these simulations is to quantify the delay caused by stop signs even when other vehicles are absent. A vehicle is simulated approaching an intersection, stopping, and then accelerating to cross straight-through. The time to cross using a stop sign is compared to the time to cross using the optimization algorithm developed here. The first simulates the optimization at a rural intersection with a speed limit of 50-MPH on each approach. The second models a more typical stop sign controlled intersection with a speed limit of 25-MPH. The vehicles use a braking angle of 37.6696^0 to decelerate, a throttle angle of 85^0 to accelerate, and each are modelled with a radius of 2.5 m. The vehicles are initially travelling at the speed limit as they approach the intersection. Table I and the corresponding data shown in Fig. 2 show the amount of additional time needed to cross the intersection because of the stop sign. The simulations demonstrate that stop signs introduce significantly more delay than the optimization algorithm.

The same scenario used to show the delay caused by a stop sign is utilized for a traffic signal as well. Determining this delay is more difficult since signal timings are often customized for specific intersections. A common configuration on low traffic roads is a fully-actuated two-phase signal. It functions by either displaying green for east-west or north-south traffic and changing only when vehicles are detected. In the case that the vehicle arrives from an approach that is already signalling green, the vehicle is not delayed at all. However, if the vehicle is coming from the approach that is signalling red, the vehicles must first come to a complete stop, wait for the signal to change from green, to yellow, to red, then green for the approach the vehicle is coming from. The delay in this case is calculated by adding the delay caused by stopping to the delay caused by waiting through the signal's yellow time [1]. The resulting delays are displayed in Table I and Fig. 2. The results demonstrate that the optimization introduces far less delay than conventional traffic signals.

TABLE I
Average Additional Delay Caused by Stop Signs and Traffic Signals Under Sparse Traffic Conditions in Comparison to the Sparse Traffic Optimization Algorithm At Various Velocities

Velocity	Delay for Stop Sign	Delay for Traffic Signal
30 MPH	6.38 s	5.19 s
35 MPH	6.79 s	5.52 s
40 MPH	7.16 s	5.83 s
46 MPH	7.51 s	6.13 s
50 MPH	7.86 s	6.43 s

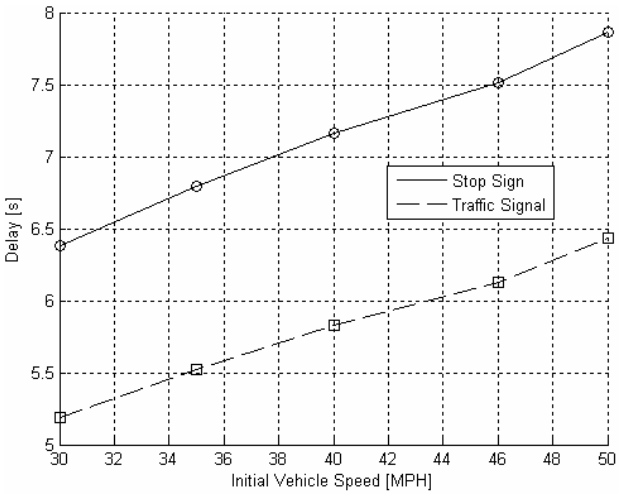

Fig. 2 Average Additional Delay Caused By Stop Signs and Traffic Signals Under Sparse Traffic Conditions In Comparison to the Sparse Traffic Optimization Algorithm At Various Speeds

VI. Conclusions

This paper has proposed a novel collision avoidance system that adapts to changing traffic conditions. The system applies a constrained coupled, EKF to estimate the states of a realistic, nonlinear, 5-state variable vehicle model. The estimates are transmitted wirelessly to other vehicles using the new WAVE standards. Vehicles use these estimates to optimize their future controls by minimizing the average vehicle delay. Results show that this cooperative intersection collision avoidance system outperforms today's common intersection control devices. The contributions of this research to the field of collision avoidance are explained followed by some avenues for future research.

The work presented here opens several research opportunities in related areas. Most vehicular optimization research focuses on minimizing time or delay. However, this optimization algorithm could be modified to account for fuel efficiency as well. Since the state space model enables the amount of fuel to be inferred from the mass of air in the intake manifold, the fuel efficiency can be studied.

There are certain aspects of the EKF that are in need of improvement before being implemented. The EKF analysis performed in this paper assumes an unconstrained filter. Future research should investigate a different method for computing the covariance matrices to reflect these constraints.

The current optimization algorithm uses an arbitrary, safe threshold to decide when to switch from sparse to dense mode. Investigating the capacity of a fully-meshed WAVE network can provide information detailing when it is appropriate to switch based on communication and processing delays as more vehicles join the network. The optimization algorithm is currently designed for four-way intersections. In the future, the algorithm could be applied to traffic circles. In order for this system to control traffic at a normal intersection, the optimization algorithm needs to be modified to account for any pedestrians. This could be accomplished by fusing optical camera and cooperatively communicated information when optimizing vehicle controls.

The optimization algorithm currently does not account for weather. During heavy precipitation, braking distances and vehicle separation need to be increased to prevent collisions. Additionally, the magnitude of the vehicle acceleration needs to be limited so that traction with the ground is not lost. Limitations in wireless communication distances also should be considered.

The decentralized, cooperative collision avoidance system presented in this paper is generally able to be implemented with today's technology. However, more work is still need to solve some of the remaining technical issues and ensure high reliability with low cost.

References

[1] A.S. Farahmand, *Cooperative Decentralized Intersection Collision Avoidance Using Extended Kalman Filtering*, M.S. thesis, Virginia Tech, December 5 2008.

[2] J.K. Hedrick, D.H. McMahon,and D. Swaroop, "Vehicle modeling and control for automated highway systems". California PATH Program, UC Berkeley, November 1993.

[3] TransSafety, Inc. "When Stop Sign Was Downed Six Times in Seventeen Days, Texas DOT May Be Liable for Not Correcting Sign's Susceptibility to Vandalism". Road Injury Prevention & Litigation Journal. June 29 2000. Last Accessed February 28 2008. <http://www.usroads.com/journals/rilj/0107/ri010701.htm>.

[4] T. Tsuji, H. Hattori, M. Watanabe, and N. Nagaoka, "Development of night-vision system". *IEEE Transactions on Intelligent Transportation Systems*, Vol. 3, No. 3, pp. 203-209, September 2002.

[5] B. Ulmer, "VITA - an autonomous road vehicle(ARV) for collision avoidance in traffic". *Proceedings of the Intelligent Vehicles Symposium*, pp.36-41, July 1992.

[6] S. Quinlan and O. Khatib, "Elastic bands: connecting path planning and control". *Proceedings of IEEE International Conference on Robotics and Automation*, Vol. 2, pp. 802-807, May 1993.

[7] P.N. Pathirana, A.E.K. Lim, A.V. Savkin, and P.D. Hodgson, "Robust video/ultrasonic fusion-based estimation for automotive applications". *IEEE Transactions on Vehicular Technology*, Vol. 56, No. 4, pp. 1631-1639, July 2007.

[8] L. Li and F.Y. Wang, "Cooperative driving at blind crossings using intervehicle communication". *IEEE Transactions on Vehicular Technology*, Vol. 55, No. 6, pp. 1712-1724, November 2006.

[9] K. Sung, J. Yoo, and D. Kim, "Collision warning system on a curved road using wireless sensor networks". *IEEE Vehicular Technology Conference*, pp. 1942-1946, September 2007.

[10] H.S. Tan and J. Huang, "DGPS-based vehicle-to-vehicle cooperative collision warning: engineering feasibility viewpoints". *IEEE Transactions on Intelligent Transportation Systems*, Vol. 7, No. 4, pp. 415-428, December 2006.